URSI GASS 2021, Rome, Italy, 28 August - 4 September 2021

Analysis of Mm-Wave Scattering from Construction Materials

M. Buccioli, E. M. Vitucci, V. Degli-Esposti
DEI, University of Bologna - 47522 Cesena, Italy, https://dei.unibo.it/en/index.html

Abstract

MM-wave frequency bands at around 27 and 38 GHz have been recently allocated to 5G communications and therefore the characterization of transmission, reflection and scattering characteristics of building materials at those frequencies is in the spotlight. Scattering from common construction materials is analysed in the paper through both directional measurements and simulations. Differently from common sentiment, it is shown that 27 GHz waves can penetrate into walls and scattering from internal structures can be relevant, especially in the case of Gypsum board dividing walls. It is shown that back-scattering can be modelled with the double lobe version of the Effective Roughness model for 3 very common construction materials, with different parameters depending on the material.

1 Introduction

Mm-wave propagation characteristics are known to be different from those of radio propagation below-6GHz, the most important aspect being the higher path-loss [1]. While this is certainly true for isotropic free-space path loss, which is proportional to the square of frequency, the same statement is not as obvious for transmission loss through a material slab, such as a wall or a concrete floor. In fact, some materials (e.g. marble or plaster) can show a quite low transmission loss even at mm-wave frequencies [2].
It is also commonly believed that mm-wave scattering due to surface roughness is stronger than surface scattering below 6 GHz, while volume scattering, i.e. the effect of dishomogeneities inside the material slab, is negligible due to the lower penetration. A few studies however have shown that surface roughness' standard deviation is almost always much lower than the wavelength and that surface scattering is not very significant, except for brick walls and rough plaster materials, even at mm-wave frequencies [3].
While there is a vast literature on the measurement of the mm-wave dielectric properties of homogeneous materials, only some recent investigations have studied overall reflection, transmission and scattering from common compound material slabs used in buildings [3]-[6], or scattering from smaller objects, which become electrically large and therefore important as the frequency increases [7]. In a few investigations diffuse scattering from building walls at mm-waves – either due to surface roughness or other phenomena - has been modeled using the Effective Roughness (ER) model [3]-[5] or the Kirchhoff model [6].

In the present work we measured scattering at 27 GHz from 3 very common construction material slabs having similar surface characteristics using a simple portable spectrum analyzer setup. Results show that volume scattering is very relevant in dishomogeneous compound materials such as a gypsum board and, to a lesser extent, a brick wall. We have then simulated scattering using the ER model and found that the double-lobe scattering-pattern version is the one giving the best results. The prominence of the back-scattered lobe becomes less relevant when moving from gypsum board to the brick wall and almost absent - as it should - for the sandstone slab, which is made of electrically homogeneous material.

2 The Measurement setup

Static measurements have been carried out on the above-mentioned samples of construction materials (sandstone slab, brick wall and Gypsum board panel) at 27 GHz and 38 GHz through a J0SSAP14 portable kit provided by SAF Tehnika, composed by a compact Signal Generator (SG) and Spectrum Analyzer (SA). The SG maximum output power is 5 dBm, while the SA can detect signals over the 26-40 GHz band with a sensitivity of about -100 dBm. The sweep time is 0.5 sec. at the minimum frequency span, i.e. two Received Signal Strength (RSS) values per second can be recorded. Circular horn antennas with a gain of about 21 dB and Half-Power Beamwidth of 15° (two-way) have been used at both link ends. The SAF Tehnika equipment and the horn antenna are shown in Figure 1.

(a) (b) (c)

Figure 1. Illustration of the portable SAF Tehnika measurement equipment: (a) Compact Signal Generator (b) Compact Spectrum Analyzer; (c) Circular horn antenna

During the measurements, Tx Power has been set to 5 dBm, and the measured data have been averaged over a time interval of 10 seconds, to minimize the effect of random fluctuations in the signal caused by the surrounding environment for each measurement location.
The measurement equipment has been calibrated in free-space in order to find additional losses with respect to Friis

equation's path-loss, caused for example by cables and connectors: this calibration is needed to properly tune the Ray Tracing model for comparison with measurements, which will be shown in Section 3. After calibration, an additional loss of 6.4 dB has been found at 27 GHz, and of 5.44 dB at 38 GHz: the 1 dB reduction at 38 GHz is probably caused by a slight increase of the antenna gain w.r.t. the nominal values reported in the datasheet, while cable losses are similar at the 2 frequencies.
In Figure 2, a detail view of the 3 considered material slabs is shown: in particular, it can be observed the structure of the brick holes (Fig. 2b), and the internal and external metal frames of the gypsum panel (Fig. 2c).
Thickness is 4 cm for the sandstone slab, and 7 cm for both the brick wall and the gypsum board.

(a) (b) (c)

Figure 2. Detail view of the material samples: a) limestone slab: we used the smooth-surface one underneath; b) brick wall c) gypsum board wall, without external gypsum layer to show part of the internal metallic structure

3 Measurement and modeling results

Scattering measurements have been carried out with the simple setup described in Section 2 by illuminating the Item Under Test (IUT) with the Tx horn antenna mounted on a mast with an angle of incidence of 45° toward the IUT centroid at a distance of 2.25 m from it (see Figure 3). Angles are measured from the IUT surface throughout this work. The Rx end has been placed on a moving table at a distance of 1.5 m from the IUT and positioned on successive points on a 140° circular arc spaced by 10°, either on the same side of the IUT for backscattering measurements or on the opposite side for forward-scattering and transmission measurements. The different positions along the arc are sketched in Figure 3 with small crosses on the ground, for the backscattering measurements. It is worth noting that with the chosen Tx/Rx distances, and discarding grazing angles in the Rx arc (from 0 to 20° and from 160° to 180°), we ensured that the whole footprint of the -6 dB lobe of antennas would fall completely within the IUT surface, in order to minimize the effect of edge diffraction.
Polarization was always vertical for both antennas in all cases reported in this paper.

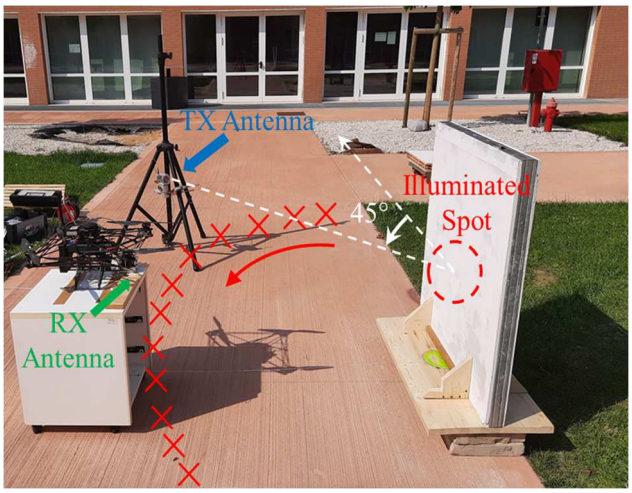

Figure 3. Illustration of the setup for backscattering measurements (Tx illumination angle: 45°).

In order to calibrate the ER diffuse scattering model, and similarly to what done in previous work [3][9], Ray Tracing (RT) simulations have been carried out using the model described in [8] exactly reproducing the measurement setup and geometric layout, including the radiation patterns of the antennas, and setting the dielectric parameters to the values which were measured on the same material samples in past work [2]. The RT model also includes the ER scattering model, which has been calibrated in order for simulation results to match measurements at best. In the ER model, it is assumed that part of the incident power is scattered at the expense of specular reflection according to the scattering parameter S, and the diffuse power is distributed according to a given scattering pattern. In [9], a double-lobe shape is hypothesized for walls/objects with large volume irregularities and indentations, and in such a case the field intensity is expressed as:

$$\left|\vec{E}_S\right|^2 = E_{S0}^2\left[K_R\left(\frac{1+\cos\psi_R}{2}\right)^{\alpha_R} + (1-K_R)\left(\frac{1+\cos\psi_i}{2}\right)^{\alpha_i}\right] \quad (1)$$

where the amplitude E_{S0} is proportional to S (in addition to other factors which are needed to ensure that total power is conserved), Ψ_R and Ψ_i are the angle deviations with respect to specular reflection direction and incidence direction, respectively, K_R is a parameter that sets power-repartition between scattering around the specular direction (near-reflection lobe), and backscattering toward the Tx direction (backscattering lobe), α_R and α_i define the width of the reflection and backscattering lobe, respectively. When K_R=1, the scattering pattern boils down to a single-lobe around specular reflection.
Measured and simulated scattering pattern results at 27 GHz are reported in Figures 4, 5 and 6 for the limestone slab, the gypsum board and the brick wall samples, respectively.
Except for the limestone slab, for the other two materials the presence of strong back-scattering in Rx locations far from specular reflection is evident, probably due to

diffraction and back-reflection effects caused by the walls' internal structures. Similar results have been obtained also at 38 GHz, not reported here for the sake of brevity. This finding is confirmed by the fact that the double lobe scattering pattern originally hypothesized in [9] and expressed by Eq. (1) gives the best results in these two cases.

The main parameters of the ER model with double-lobe pattern have then been calibrated to find the best match with measurements. In order to simplify the optimization procedure, the same value $\alpha=\alpha_R=\alpha_i$ has been fixed for the angular amplitude of the reflection and back-scattering lobes: in particular, the value $\alpha=3$ has been assumed, which gave the best results in previous work for typical building walls and construction materials [7,9].

The best-fit parameter K_R (named Λ in [9]) is equal to 0.5 for the brick wall, meaning that diffuse power is equally divided between the two lobes, and equal to 0.3 for the Gypsum board, meaning that in the latter case 70% of the diffuse power is steered in the backscattering direction. On the other hand, K_R is equal to 1 for sandstone, which means, there is no relevant backward diffuse scattering in this case. The scattering parameter S, on the contrary, shows an opposite trend, i.e. diffuse scattering power relative to specular reflected power is minimum for sandstone and maximum for the gypsum board.

The best-fit parameters for the ER model and the RMS Error of simulations w.r.t. measurements are summarized in Table I.

As for transmission (or insertion) loss L_τ for normal incidence, after averaging 5 measurements with slightly different incidence angles to get rid of multipath fading effects, which were probably due to the above-mentioned internal structures, we got the following results: 17 dB, 15.2 dB and 4.7 dB for limestone, bricks and gypsum board, respectively (see Table II).

The foregoing results are quite interesting and basically show that volume scattering is quite relevant in the 26-40 GHz frequency band, and becomes severe for light, low-loss materials with internal dishomogeneities such as the gypsum board. The main origin of diffuse scattering in the considered cases cannot be surface roughness since all three materials have similar, smooth surfaces. It is worth noting that the best-fit RMSE, low for the first two cases, is sensibly higher for the gypsum board, due to the deep saddle of the curve between 80 and 100 degrees, which the ER model cannot reproduce well. Probably, a different parametrization or a different formulation with a more directive back-scattering lobe should be used for this case.

TABLE I – Best-fit parameters of ER Scattering Model in the backward scattering case at 27 GHz

Material	Best-fit S	Best-fit K_R	Best-fit RMSE (dB)
Sandstone	0.2	1	3.24
Brick wall	0.3	0.5	3.55
Gypsum board	0.4	0.3	6.42

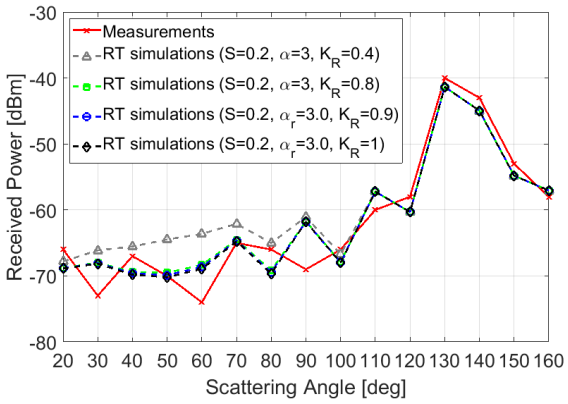

Figure 4. Sandstone sample: measurement vs simulation comparison for different value of the K_R parameter

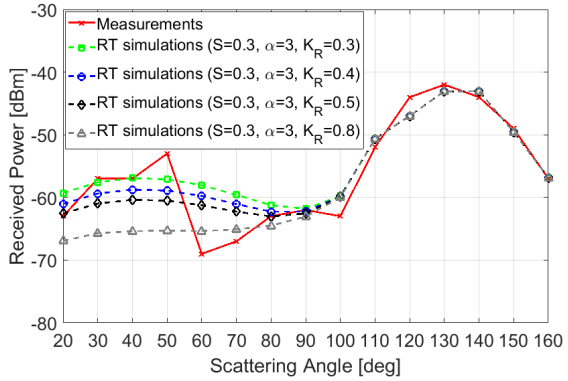

Figure 5. Brick wall sample: measurement vs simulation comparison for different value of the K_R parameter

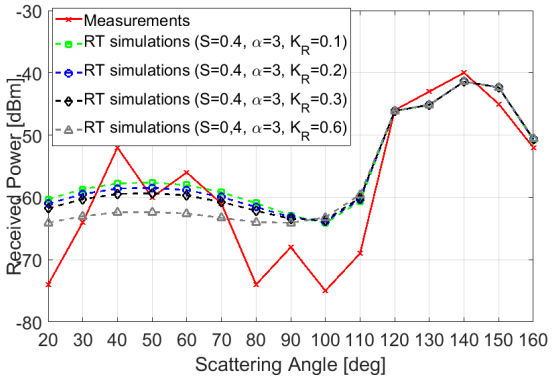

Figure 6. Gypsum board sample: measurement vs simulation comparison for different value of the K_R parameter

TABLE II – Measured transmission loss for the 3 material samples

	Sandstone	Brick wall	Gypsum board
Loss (dB)	17	15.2	4.7

4 Concluding remarks

Scattering from some common construction materials at 27 GHz is analysed in the paper through both directional measurements and simulations. Differently from common sentiment, it is shown that scattering from internal structures can be relevant, especially in the case of Gypsum-board dividing-walls which have a low penetration loss and relevant internal dishomogeneities.
Results also show that probably, a different model with a more directive back-scattering lobe should be used for this case. Back-ward diffuse scattering is also evident for the brick wall, that together with gypsum board represents by far the most common type of diving wall used worldwide.
More materials samples, mm-wave frequency bands and polarization cases will be object of future investigations.

5 References

1. S. Salous et al., "Millimeter-Wave Propagation: Characterization and modeling toward fifth-generation systems. [Wireless Corner]," in IEEE Antennas and Propagation Magazine, vol. 58, no. 6, pp. 115-127, Dec. 2016

2. L. Possenti, J. Pascual Garcia, V. Degli-Esposti, A. Lozano Guerrero, M. Barbiroli, M. T. Martinez-Inglés, F. Fuschini, J. V. Rodríguez, E. M. Vitucci, J. M. Molina-García-Pardo, "Improved Fabry-Pérot Electromagnetic Material Characterization: Application and Results," Radio Science, 55, e2020RS007164, 2020.

3. J. Pascual-García, J. Molina-García-Pardo, M. Martínez-Inglés, J. Rodríguez and N. Saurín-Serrano, "On the Importance of Diffuse Scattering Model Parameterization in Indoor Wireless Channels at mm-Wave Frequencies," in IEEE Access, vol. 4, pp. 688-701, 2016.

4. X. Liao, Y. Shao, Y. Wang and T. Hu, "Experimental Study of Diffuse Scattering from Typical Construction Materials over 40-50GHz," 2018 IEEE Asia-Pacific Conference on Antennas and Propagation (APCAP), Auckland, 2018, pp. 216-218.

5. E. M. Vitucci, J. Chen, V. Degli-Esposti, J. S. Lu, H. L. Bertoni and X. Yin, "Analyzing Radio Scattering Caused by Various Building Elements Using mm-Wave Scale Model Measurements and Ray-Tracing," IEEE Transactions on Antennas and Propagation, Vol. 67 No. 01, January 2019

6. M. Jung, J. Kim, Y. Yoon, J. Kim and S. Kim, "Enhancement approach of ray-tracing algorithm for propagation prediction at the MM-wave band," 35th International Conference on Infrared, Millimeter, and Terahertz Waves, Rome, 2010, pp. 1-2.

7. F. Fuschini, S. Hafner, M. Zoli, R. Muller, E. M. Vitucci, D. Dupleich, M. Barbiroli, J. Luo, E. Schulz, V. Degli-Esposti, R. S. Thomä, "Item Level Characterization of mm-wave Indoor Propagation," Eurasip Journal on Wireless Communications and Networking, January 2016

8. F. Fuschini, E. M. Vitucci, M. Barbiroli, G. Falciasecca, V. Degli-Esposti, "Ray tracing propagation modeling for future small-cell and indoor applications: a review of current techniques," Radio Science, Volume 50, Issue 6, Pages: 469–485, June 2015

9. V. Degli-Esposti, F. Fuschini, E. Vitucci, G. Falciasecca, "Measurement and modelling of scattering from buildings", IEEE Transactions on Antennas and Propagation, Vol. 55 No 1, pp. 143-153, January 2007